A Study of the Effect of Precipitated Austenite on the Fracture of a Ferritic Cryogenic Steel

DARREL FREAR and J. W. MORRIS, Jr.

The effect of precipitated austenite on the fracture of an Fe-8Ni-2Mn-0.1Ti steel was investigated. The study attempted to correlate microstructure, mechanical properties, and the fracture surface appearance of specimens heat treated to contain austenite or to be austenite free. The fracture surfaces were quantitatively studied using a 3D imaging technique in the SEM. It was found that the presence of austenite had a beneficial influence of lowering the ductile-to-brittle transition temperature. Part of this decrease was found to be due to the austenite gettering deleterious elements off the grain boundaries. Specimens that contained precipitated austenite were also found to have a smaller median facet size, when fractured in a brittle transgranular mode, than specimens with no austenite. The smaller facet size is shown to be associated with a decrease in ductile-to-brittle temperature.

I. INTRODUCTION

IT is desirable to use ferritic steels at low temperatures because of their low cost. Ferritic steels also offer a good strength/toughness combination provided that the service temperature is above the ductile-to-brittle transition temperature (T_B). A great deal of research has been done with the goal of decreasing the T_B. The research has followed two paths in the attempt to lower the T_B of ferritic Ni steel. The first involves refining the grain size of the steel.[1-4] This approach has been used to process a 12Ni steel so that it is ductile down to 4 K.[5] The second line of research, and the topic of this paper, involves the addition of precipitated austenite to the ferritic matrix.[6]

It is generally agreed that the precipitated austenite must be thermally stable to have a beneficial influence on cryogenic properties.[7] However, several hypotheses have been proposed to explain how the precipitated austenite lowers the T_B. These hypotheses include:

Austenite acting as a crack blunter.[8,9,10] This hypothesis is based on the assumption that a crack propagating through the steel would blunt in the ductile fcc austenite. However, Fultz and Morris,[11] and Kim and Schwartz[12] have shown that the austenite is mechanically unstable and transforms to martensite in front of the crack tip. Recent work by Kim, *et al.*[13] has shown that the austenite is in fact brittle and could not blunt the crack.

Austenite scavenging deleterious elements.[7,14] The austenite acts as a sink for grain boundary pollutants, such as P and S, and the toughness is increased by eliminating intergranular fracture.

Crystallographic cleavage impairment model.[6] The austenite transforms to a variant of martensite that corresponds to the highly strained region in front of the crack tip. It is probable that this new variant of martensite is different from the matrix[15] and thus creates a high angle boundary. Upon brittle fracture the fracture surface would consist of smaller facets due to the presence of the mechanically transformed austenite. This smaller facet size has been seen qualitatively but has not been quantitatively measured. By creating more high angle boundaries the initiation of cleavage cracks becomes more difficult and thus lowers the T_B much in the same way that refining the grain size accomplishes the same result.

This work was designed to investigate the function that austenite has in the fracture of a ferritic steel. This investigation has a threefold purpose: (1) to measure quantitatively the facet size on the brittle fracture surfaces of a ferritic steel that contains austenite and compare these results to specimens that contain no austenite, (2) to investigate whether the presence of austenite alone will lower the T_B, and (3) to determine the effect the tempering treatment has on the yield strength.

An alloy of nominal 8Ni-2Mn-0.1Ti steel was chosen for this investigation because previous work[3] on this same alloy showed that an intercritical temper would precipitate out an even distribution of austenite. A low carbon content was desired because the carbides that form add a complicating factor to both the microstructure and mechanical properties[16] confusing the effect that the austenite has on the steel. The small amount of Ti was added to getter any carbon that happens to be present.

The QLT heat treatment,[18] a heat treatment developed for commercial cryogenic steels (Figure 1), was chosen to observe the effects of the precipitated austenite by comparing samples with and without austenite. The Q is a single phase γ heat treatment at 750 °C for 1 hour followed by an ice water quench. The QL treatment at 660 °C for 1 hour is an intercritical anneal high in the 2-phase region so any γ that forms is low in solute content and should be thermally unstable. Both of these heat treatments should contain no precipitated austenite. The QT and QLT specimens were designed to contain thermally stable precipitated austenite that forms during the T (12 hours at 550 °C) intercritical temper.

II. EXPERIMENTAL PROCEDURE

An alloy of nominal Fe-8Ni-2Mn-0.1Ti steel was induction melted in an inert argon gas atmosphere. The composition in weight percent was Fe-7.95Ni-1.93Mn-0.07Ti-0.003N-0.0040-0.003P-0.003S-<0.001C. The alloy

DARREL FREAR, Graduate Research Student Assistant, Lawrence Berkeley Laboratory, and J. W. MORRIS, Jr., Professor of Metallurgy, are with The University of California, Berkeley, CA 94720.

Manuscript submitted January 14, 1985.

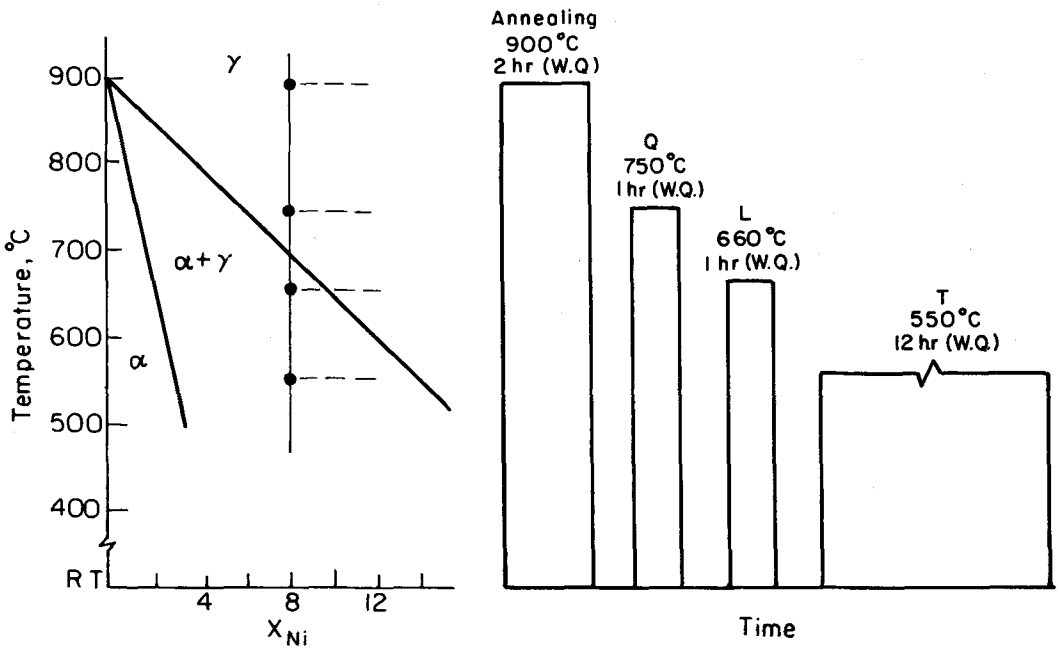

Fig. 1 — Schematic diagram showing heat treatment times and temperatures along with the relevant portion of the phase diagram.

was homogenized at 1200 °C for 24 hours, and then hot rolled into 0.5 inch (12.7 mm) plates. The heat treatment used in this investigation is based on a modified version of the conventional QLT heat treatment.[17] In addition to the QLT treatment three variations were also made and will be referred to as: Q, QL, and QT. These heat treatments are diagrammed in Figure 1.

The microstructure was characterized in TEM using a Phillips EM 301 operated at 100 kV. An X-ray diffraction analysis was used to determine the volume fraction of precipitated austenite phase. Impact toughness results were obtained using the ASTM standard Charpy v-notch specimens. Tensile tests were performed using subsized flat tensile specimens. Both impact and tensile tests were done at temperatures ranging between liquid nitrogen and room temperature in a bath mixture of liquid nitrogen and isopentane. Impact tests at liquid helium were performed using the styrofoam box method developed by Jin, *et al.*[2]

The fracture surfaces of broken Charpy specimens were observed using a JEOL JSM-U5 SEM operated at 20 kV. In order to determine the facet size on the brittle fracture surfaces of the Charpy specimens it was necessary to take stereo fractographs tilting the specimen about an axis to image the facets in three dimensions.[18] The true facet size was determined by digitizing the information off the stereo micrographs on a Calcomp 9000 digitizer. The data were then processed using a computer interfaced to the digitizer. To be able to get the true facet size a three-dimensional technique was used where it is possible to determine the actual dimensions of the facets by tilting the specimen so an image in three dimensions may be made. This makes it possible to determine the angle between the facet and the fracture surface plane and measure the true facet dimension. A schematic diagram of this procedure is given in Figure 2. For this work it is necessary to have a definition of a facet

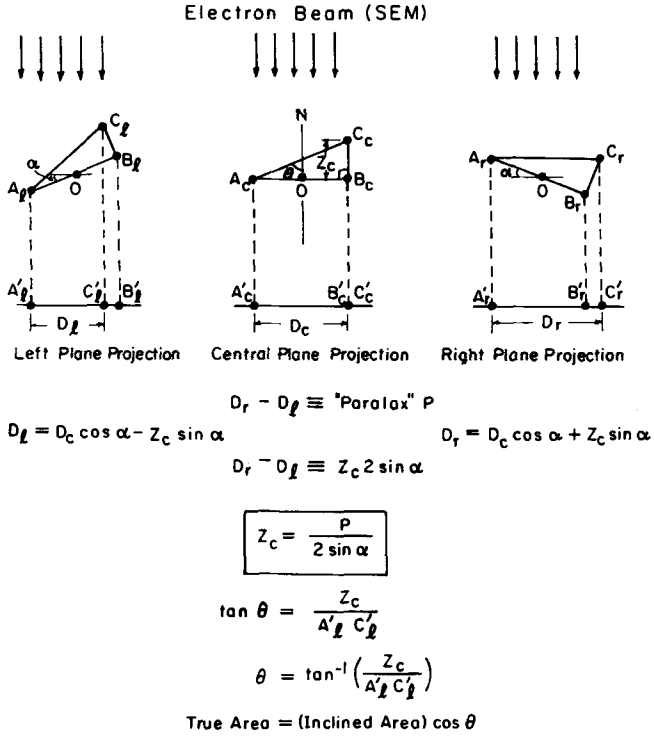

Fig. 2 — Geometry of specimen tilting in the SEM to create a 3D image.

to keep the measurements objective. A facet is here defined as being a flat region, on a brittle fracture surface, that has river patterns running across it. To get good statistics approximately 1000 facets were measured for each heat treatment using four broken Charpy specimens per heat treatment.

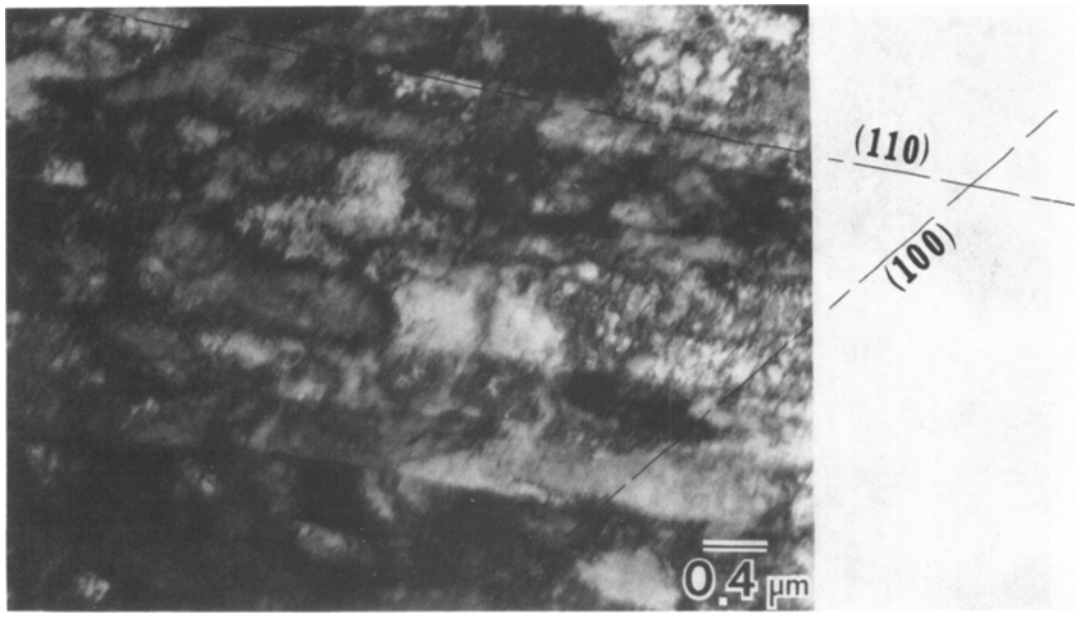

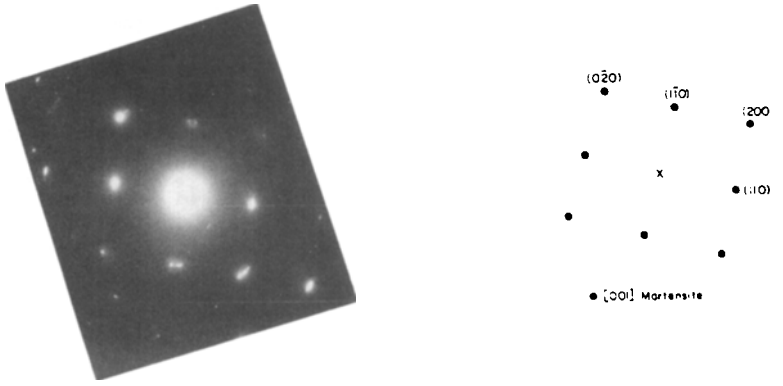

Fig. 3—TEM micrograph of lath microstructure showing (110) lath plane and (100) cleavage plane.

III. RESULTS AND DISCUSSION

A. *Microstructure*

The microstructure of the alloy in the Q condition is shown in Figure 3 and is a highly dislocated lath martensite. There is no retained austenite present. The laths are separated by low angle boundaries and give a single diffraction pattern, in accord with Morris *et al.*,[6] Wayman,[19] and Naylor.[15] The similarly oriented laths lie in packets within prior austenite grain boundaries. The packet boundaries are of a high angle nature. Figure 3 also shows that the laths usually are parallel to (110) and the common cleavage plane, (100), is translath.

The QL microstructure is shown in Figure 4. In this heat treatment the martensitic steel was intercritically annealed for 1 hour and then quenched. During the intercritical annealing the steel has both α and γ present, but upon quenching the γ phase transforms to highly dislocated martensite upon quenching. This transformed austenite has the same variant as the surrounding packet so no new high angle boundaries are formed. The diffraction pattern in Figure 4 shows a single variant in a region that contains both matrix and thermally transformed austenite. The dark fuzzy regions in Figure 4 appear to be austenite that has transformed to highly dislocated martensite. The matrix of the QL specimen has undergone polygonization and recovery so the lath structure is replaced with polygonized subgrains that have low angle boundaries within packets. Also many of the dislocations within the subgrains have been recovered.

Figure 5 is a typical example of the QT microstructure. The bright/dark-field micrograph shows precipitated austenite and was taken from the $(200)_\gamma$ spot. The material was intercritically tempered for 12 hours at 550 °C. The austenite that has precipitated is solute rich, and therefore thermally stable down to 77 K, resulting in 6 pct austenite. The austenite is elongated and lies along {110} matrix planes. It

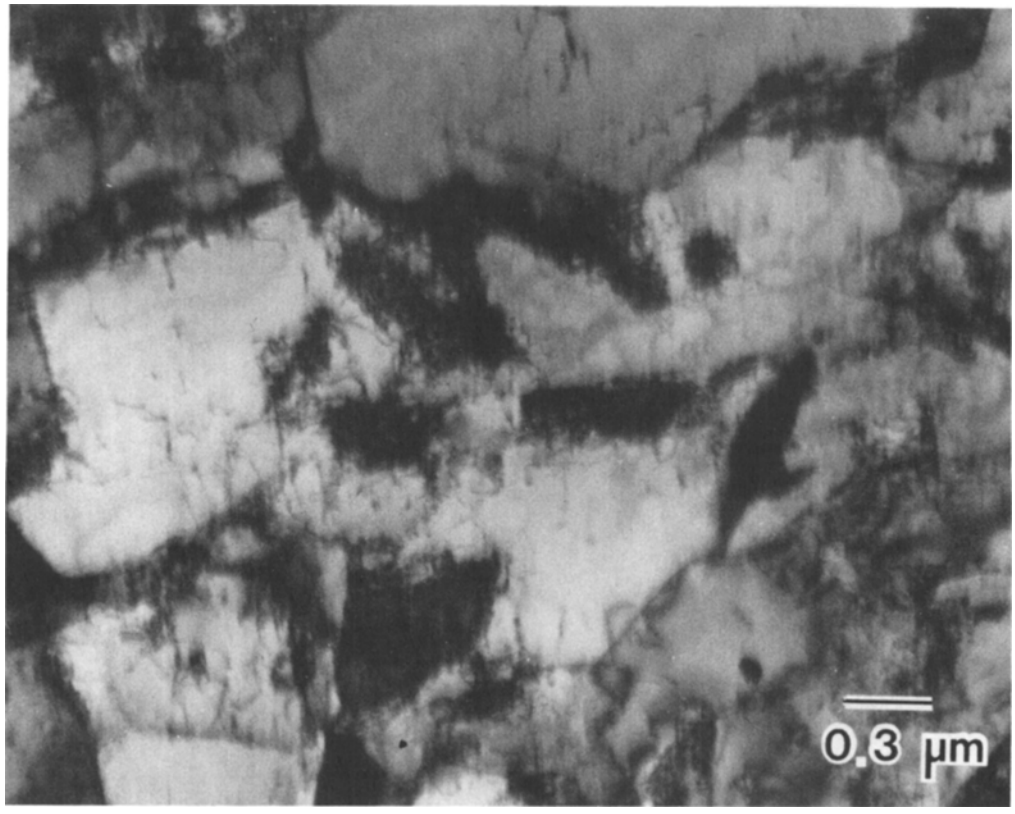

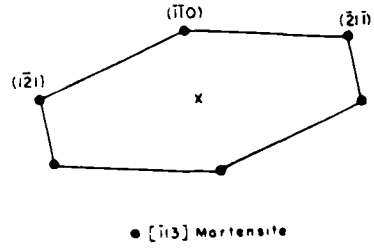

Fig. 4 — TEM micrograph of intercritically annealed (QL) specimen.

forms in both the K-S[20] and N-W[21] orientation relationships. The QT matrix has undergone recovery and polygonization but not to the same extent as in the QL condition. Quite a few dislocations are present in the matrix.

An example of the QLT microstructure is shown in Figure 6. The QLT heat treatment adds an intercritical temper to the QL microstructure forming 10 pct austenite that is thermally stable down to 77 K. The difference in volume percent of austenite between the QT and QLT heat treatments is due to the intercritical annealing step in QLT where solute-rich regions form during the treatment. The austenite precipitates from the solute-rich islands during the temper (T). The austenite in QLT has the same distribution as in QT but has a slightly larger size. The orientation relationship of the austenite in the matrix is the same for QLT as QT. The matrix of the QLT specimens has undergone extensive polygonization and recovery.

An optical microscopy study of the four heat treatments is given in Figure 7. The irregular boundaries seen in the micrographs appear to be packet boundaries. The size of the packets is similar for all the heat treatments.

B. *Mechanical Properties*

The results of the Charpy impact tests are plotted in Figure 8. The first notable point is that the upper shelf

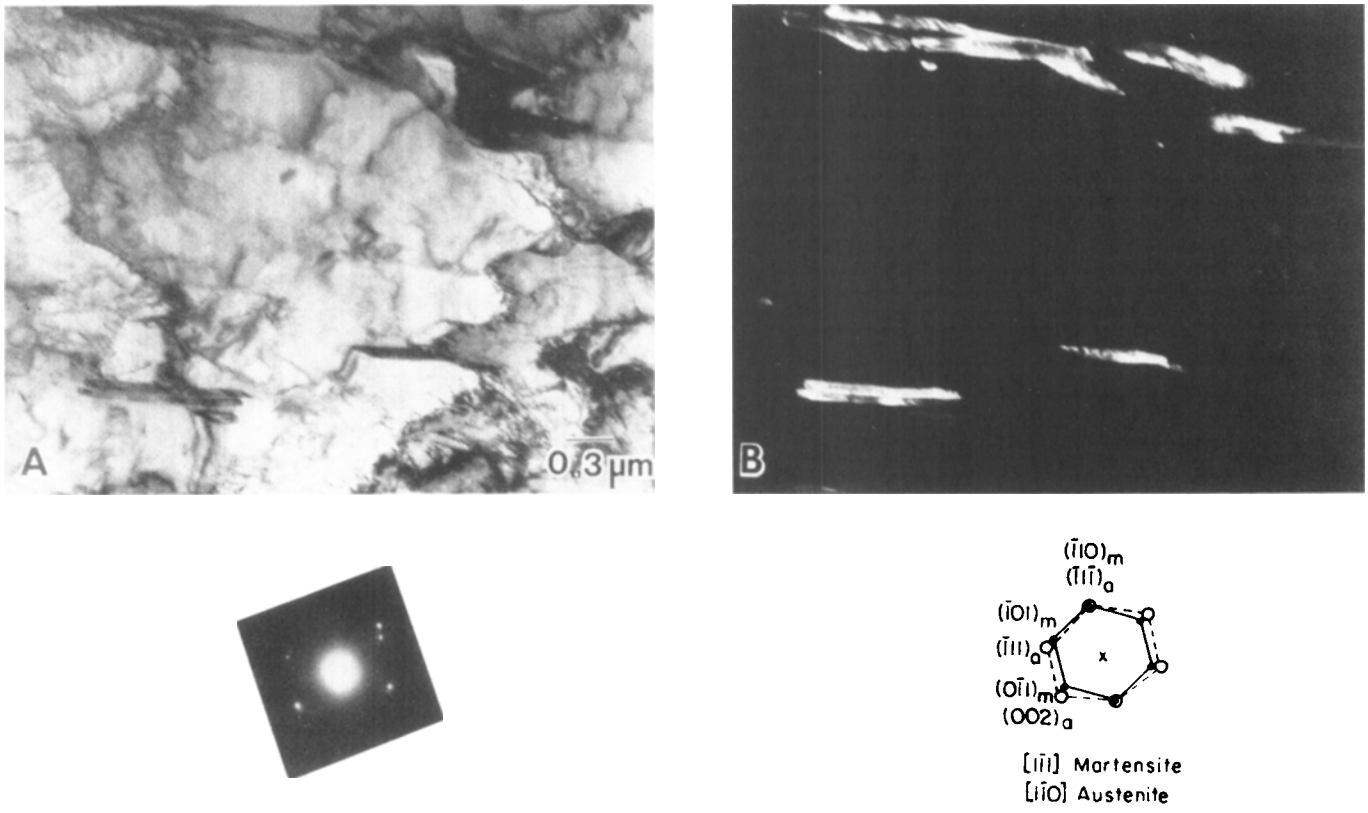

Fig. 5 — TEM micrograph of intercritically tempered (QT) specimen: (*a*) bright-field image; (*b*) dark-field contrast of austenite.

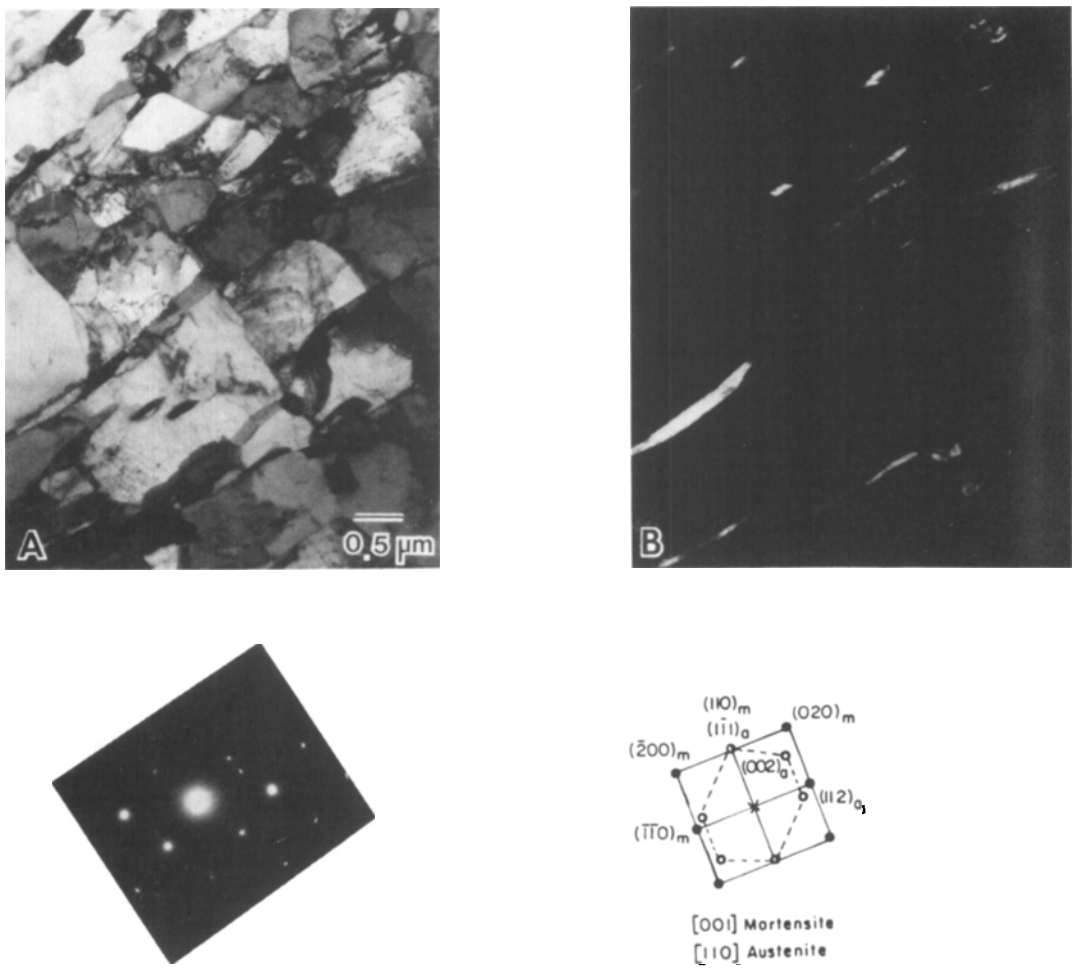

Fig. 6 — TEM micrograph of QLT specimen: (*a*) bright-field image; (*b*) dark-field contrast showing the distribution of austenite.

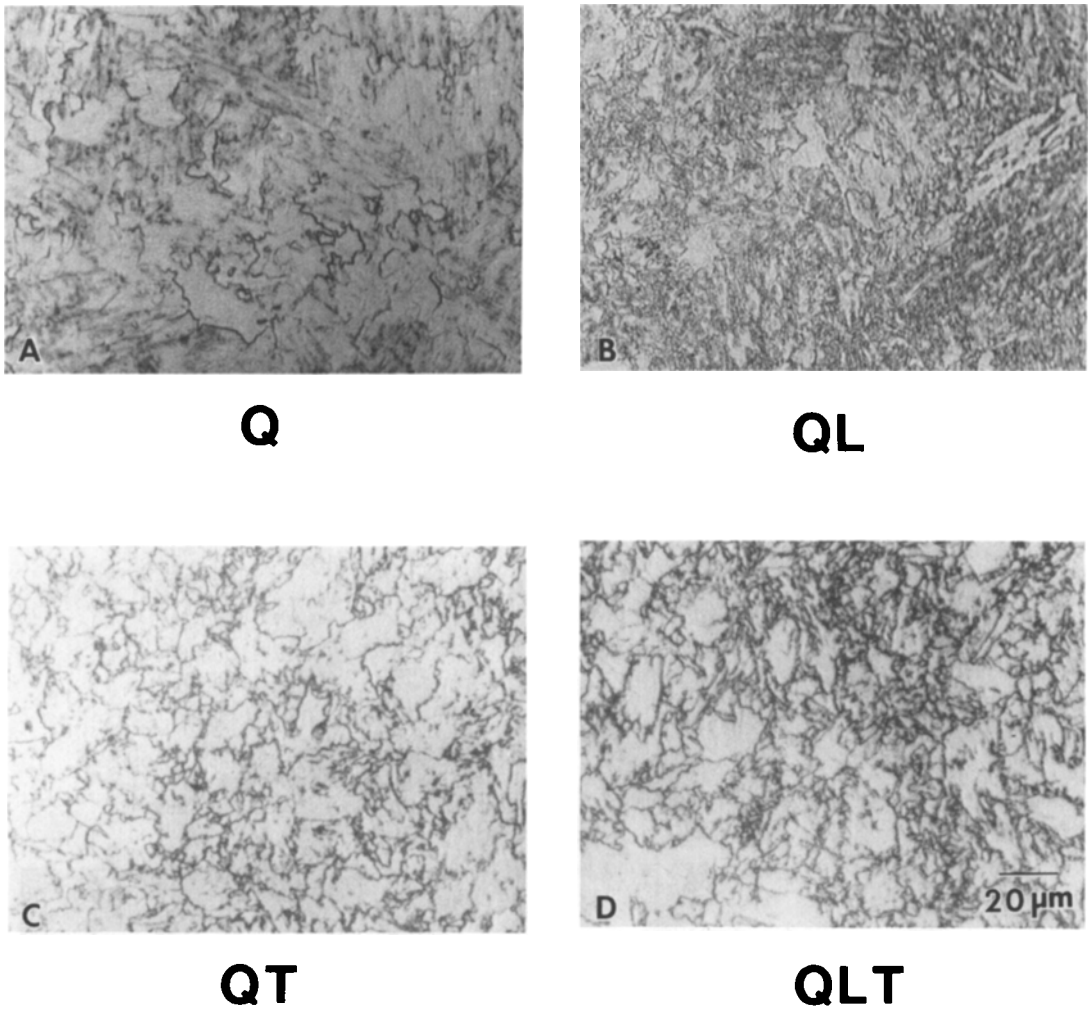

Fig. 7 — Optical micrographs of specimens as a function of heat treatment. Nital etch.

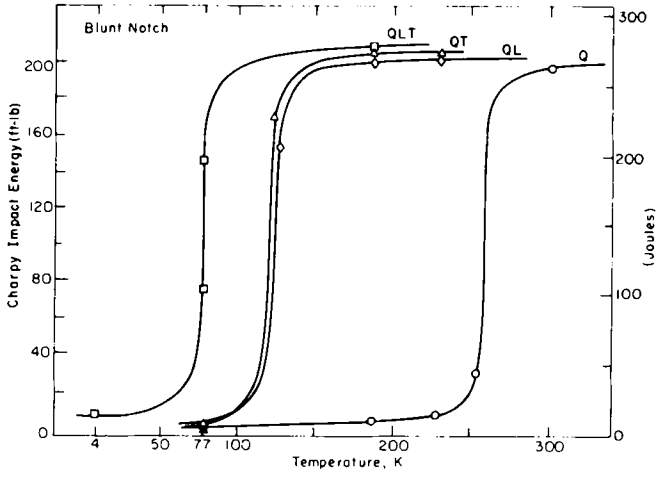

Fig. 8 — Ductile-to-brittle transition curves as a function of heat treatment for blunt notch Charpy specimens.

energies are similar. The addition of austenite has no significant effect on the upper shelf energy in this Ti-gettered steel. This contrasts with the significant change in the upper shelf on tempering steels that contain carbides.[16]

Since the transition temperatures of the austenite containing samples (QT and QLT) are the lowest, the Charpy test results suggest that precipitated austenite has an affect on the T_B.

To identify the role of the yield strength on the T_B, tensile tests were performed on flat tensile specimens at various temperatures between 77 K and room temperature. The results plotted in Figure 9 show that Q has the highest yield strength followed by QT, QL, and QLT. The yield strength appears to vary with dislocation density. The highly dislocated lath martensite of the Q condition has the largest yield strength while the greatly recovered ferrite of QLT has the lowest. The yield strength is higher in QT than QL which implies that recovery occurs to a greater extent after 1 hour at 660 °C than 12 hours at 550 °C.

The difference in yield strength between QL and QT is also relevant to the T_B shifts. A low yield strength promotes a low T_B and *vice versa*. However, QT has a lower T_B than QL despite its higher yield strength which suggests the precipitated austenite affects the T_B.

C. *Fracture Surface Analysis*

The brittle fracture surfaces were characterized by quantitative fractography to determine if the addition of austenite

influences facet size. Figure 10 shows typical brittle fracture surfaces of the four heat treatments.

In the Q condition approximately 40 pct of the fracture surface is intergranular as shown by the arrows in Figure 10(a). The intergranular fracture promotes the high T_B in the Q condition. This intergranular fracture appears to be caused by phosphorus segregation. A Scanning Auger Microscopic analysis of the fracture surface is shown in Figure 11. The specimen was broken *in situ* at 77 K and the Auger analysis was taken from an intergranular region. It was determined that there is 60 times the amount of P present at the intergranular regions as in the bulk. Phosphorus must then segregate to the austenite grain boundaries during the austenitizing treatment and cause intergranular fracture, as is well documented.[22,23,24] Despite this intergranular fracture there are also large transgranular facets present on the fracture surface. However, these facets were not measured quantitatively due to the intrusion of intergranular fracture.

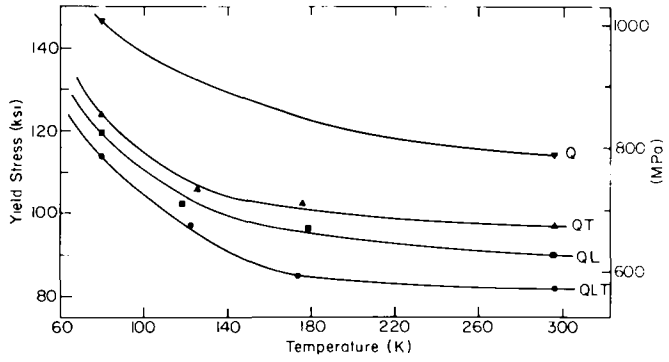

Fig. 9—Yield stress for the various heat treatments as a function of temperature.

The brittle fracture surfaces of QL, QT, and QLT show solely transgranular fracture. It is likely that the phosphorus found on the grain boundaries in the Q condition has segregated during the intercritical annealing or tempering, most likely into the austenite that has formed. The solubility of solute elements in austenite is known to be high[7,14] so the formation of austenite, whether it is thermally stable or not, provides a sink for deleterious elements such as P.

The results of the quantitative analysis of the fracture surfaces are presented as histograms in Figure 12. Comparing the three histograms, QL has an even distribution of facet areas whereas QT and QLT have the majority of facets at the lower end of facet areas. The median values for

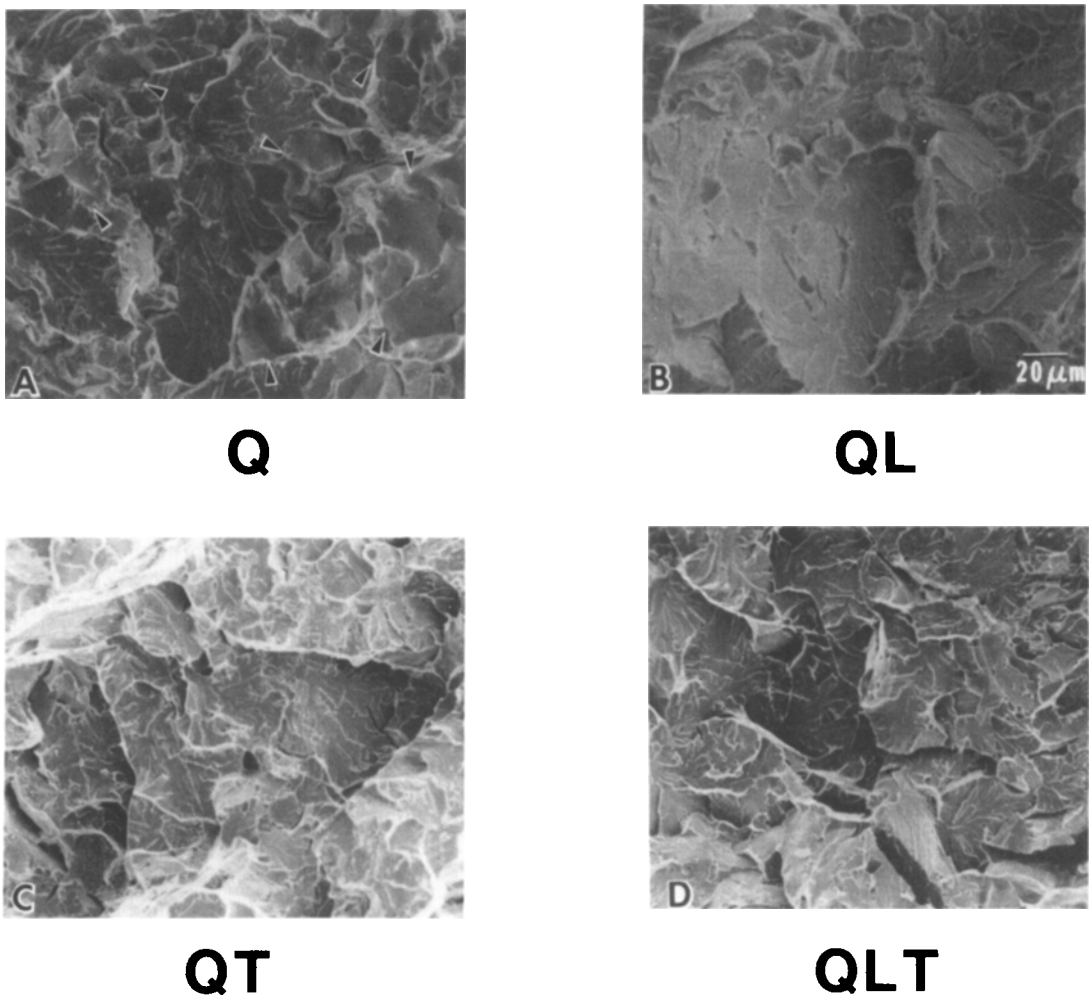

Fig. 10—SEM fractographs of the brittle fracture surfaces as a function of heat treatment.

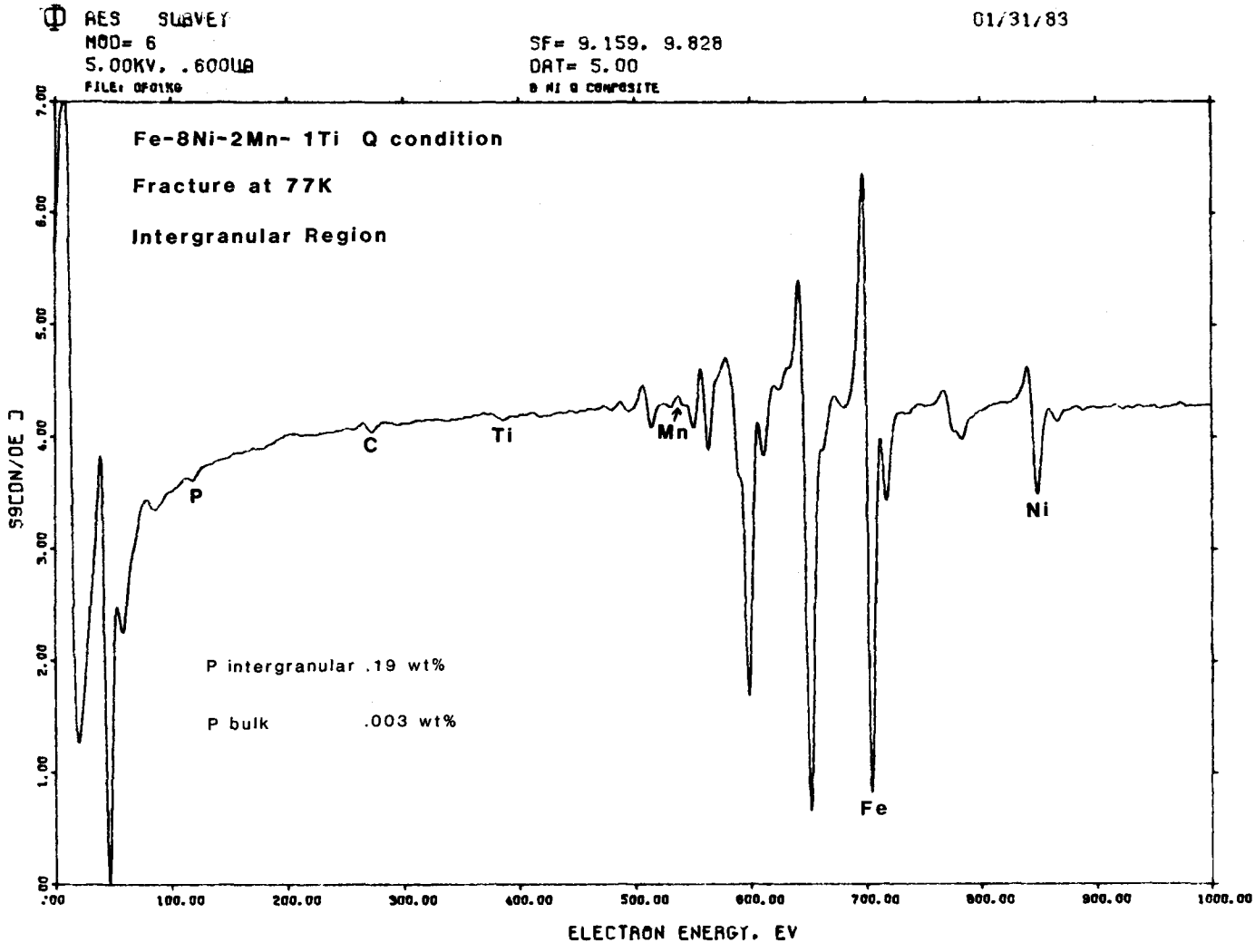

Fig. 11 — Auger electron spectrum of the brittle intergranular as-quenched (Q) specimen.

each heat treatment are: QL = 560 μm^2, QT = 225 μm^2, QLT = 219 μm^2. The median value is used because it is not influenced by an anomalous large or small number as the mean value can be. The median facet size in the QL condition corresponds very closely to the size of the packets seen in the optical microstructure of Figure 7. Therefore the facet size of the steel that contains no austenite corresponds to the packet size, as has been previously found.[15,25]

It is obvious from the above results that the presence of austenite does decrease the facet size. This correlates fairly well with an analysis of the distribution of austenite in QT and QLT from a large number of TEM micrographs. As stated previously the distribution of austenite in QT and QLT is similar, only the size of the particles differs. The median distance between austenite particles in TEM using a linear intercept method running a line along the (100) planes in bright field was found to be about 11 μm. Taking the square root of the median facet size for QT and QLT and taking it as the distance traveled between high angle boundaries results in QT = 15 μm and QLT = 14.8 μm. Therefore there is good agreement between the median crack path length and the distribution of austenite in the matrix. (The discrepancy between the facet results and TEM measurements arises, at least in part, from the difficulty of obtaining a large number of low magnification TEM micrographs that show the distribution of austenite because it is difficult to create large thin areas on the sample foils.)

The results of a decreased facet size and crack length corresponding to the austenite distribution are evidence that high angle boundaries form where the austenite has precipitated and mechanically transformed. This, combined with the results of the mechanical tests, indicates that the decrease in facet size is associated with a decrease in T_B.

IV. CONCLUSIONS

The function of precipitated austenite in an 8Ni-2Mn-0.1Ti ferritic steel was investigated. The steel was characterized by its microstructure and mechanical properties along with a study of the brittle fracture surface appearance.

The as-quenched (Q) specimens fractured in an intergranular manner that was found to be due to an enrichment of P at the grain boundaries. The heat treatments that involved intercritical annealing and tempering eliminated intergranular fracture by the precipitated austenite gettering deleterious elements.

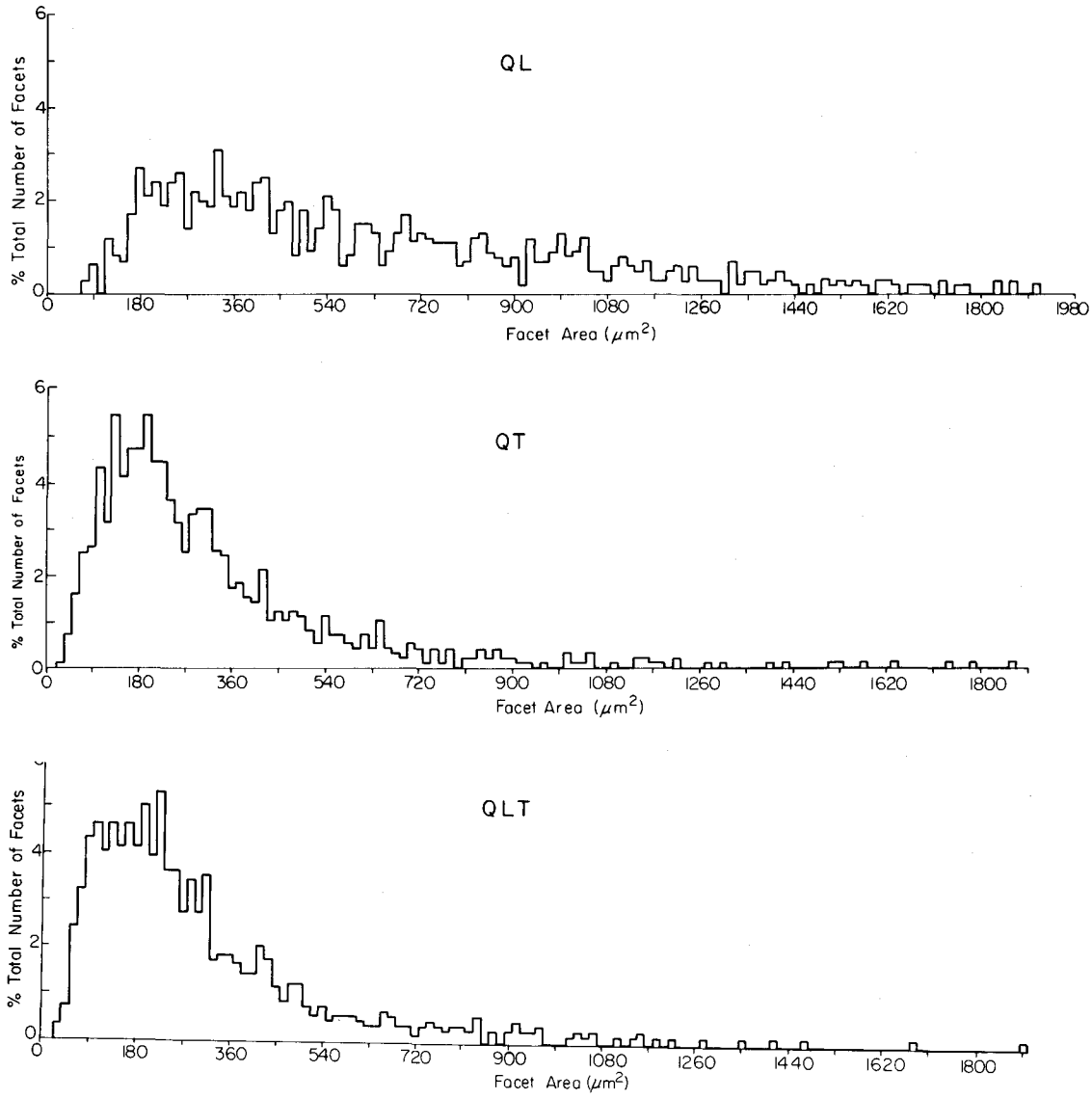

Fig. 12—Histogram plots showing facet size distribution as a function of heat treatment.

By intercritical tempering and annealing the yield strengths of the specimens varied according to heat treatment. This was thought to be due to changes in the dislocation density in the specimens created by the polygonization and recovery process.

The addition of thermally stable precipitated austenite was found to reduce the median facet size by almost half from specimens that contained no austenite. The diameter of the facets was found to correspond to the separation of the austenite precipitates in the matrix. This is evidence that the austenite transforms mechanically to a high angle boundary, in accord with the crystallographic cleavage impairment model. The decrease in facet size was also found to correspond to a decrease in the T_B.

ACKNOWLEDGMENT

This work was supported by the Director, Office of Energy Research, Office of Basic Energy Sciences, Materials Sciences Division of the United States Department of Energy under Contract #DE-AC03-76SF00098.

REFERENCES

1. S. Jin, J. W. Morris, Jr., and V. F. Zackay: *Metall. Trans. A*, 1975, vol. 6A, p. 141.
2. S. Jin, S. K. Hwang, and J. W. Morris, Jr.: *Metall. Trans. A*, 1975, vol. 6A, p. 1569.
3. S. Jin, S. K. Hwang, and J. W. Morris, Jr.: *Metall. Trans. A*, 1975, vol. 6A, p. 1121.
4. C. Syn, S. Jin, and J. W. Morris, Jr.: *Metall. Trans. A*, 1976, vol. 7A, p. 1827.
5. S. Jin, J. W. Morris, Jr., and V. F. Zackay: *Advances in Cryogenic Engineering*, 1974, vol. 19, p. 379.
6. J. W. Morris, Jr., C. K. Syn, J. Kim, and B. Fultz: *Proceedings of the International Conference on Martensitic Transformations*, MIT, Cambridge, MA, 1979, p. 572.
7. C. W. Marshall, R. H. Hehemann, and A. R. Troiano: *Trans. ASM*, 1962, vol. 55, p. 135.
8. H. J. Rack and D. Kalish: *Metall. Trans.*, 1971, vol. 2, p. 3011.
9. C. N. Alquist: *Acta Metall.*, 1975, vol. 23, p. 239.
10. O. Tamate: *Int. J. Frac. Mech.*, 1968, vol. 4, p. 257.
11. B. Fultz and J. W. Morris, Jr.: *Metall. Trans. A*, 1985, vol. 16A, p. 2251.
12. K. J. Kim and C. H. Schwartz: *Mater. Sci. Eng.*, 1978, vol. 33, p. 5.
13. J. Kim: *Metall. Trans. A*, 1985, vol. 16A, p. 2072.
14. J. Kim and J. W. Morris, Jr.: *Metall. Trans. A*, 1980, vol. 11A, p. 1401.
15. J. P. Naylor: *Metall. Trans. A*, 1979, vol. 10A, p. 861.

16. J. Kim and J. W. Morris, Jr.: *Metall. Trans. A*, 1980, vol. 11A, p. 1401.
17. S. Yano, H. Sakuri, H. Mimura, N. Wakita, T. Ozawa, and K. Aori: *Trans. ISIJ*, 1973, vol. 13, p. 133.
18. A. Boyd and P. G. T. Howell: *Scanning Electron Microscopy*, 1977, vol. 1, p. 571.
19. B. P. J. Sandvik and C. M. Wayman: *Metall. Trans. A*, 1983, vol. 14A, p. 809.
20. B. Kurjomov and G. Sachs: *Z. Physik*, 1930, vol. 64, p. 325.
21. Z. Nishiyama: *Martensitic Transformations*, Academic Press, New York, NY, 1978, p. 8.
22. R. O. Ritchie: *Metall. Trans. A*, 1977, vol. 8A, p. 1131.
23. T. Matsuyama and H. Suto: *Trans. JIM*, 1979, vol. 20, p. 44.
24. S. Yu and C. J. McMahon, Jr.: *Metall. Trans. A*, 1980, vol. 11A, p. 277.
25. J. P. Naylor and P. R. Krahe: *Metall. Trans. A*, 1975, vol. 6A, p. 594.